Marine Pollution Bulletin 211 (2025) 117470

ELSEVIER

Contents lists available at ScienceDirect

Marine Pollution Bulletin

journal homepage: www.elsevier.com/locate/marpolbul

# Extreme abiotics drive sediment biocomplexity along pH gradients in a shallow submarine volcanic vent

C. Andolina [a,b,c,1], G. Cilluffo [a,b,c,*,1], V. Zammuto [c,d,1], G. Signa [a,b,c], M. Papale [c,e], A. Lo Giudice [b,e], R. Di Leonardo [a], V. Costa [f], L. Ciriminna [a,c], A. Tomasello [a,b,c], C. Gugliandolo [c,d], S. Vizzini [a,b,c]

[a] Department of Earth and Marine Sciences, University of Palermo, via Archirafi 18, 90123 Palermo, Italy
[b] National Biodiversity Future Center (NBFC), Piazza Marina 61, 90133 Palermo, Italy
[c] CoNISMa, National Interuniversity Consortium for Marine Sciences, Piazzale Flaminio 9, 00196 Roma, Italy
[d] Department of Chemical, Biological, Pharmacological and Environmental Sciences, University of Messina, V.le Stagno d'Alcontres, 31, 98166 Messina, Italy
[e] Institute of Polar Sciences, National Research Council (CNR-ISP), Spianata San Raineri 86, 98122 Messina, Italy
[f] Department of Integrative Marine Ecology (EMI), Stazione Zoologica Anton Dohrn, CRIMAC, Calabria Marine Centre, Amendolara, Italy

ARTICLE INFO

*Keywords:*
Ocean acidification
Prokaryotic community
Stable isotopes
Carbon
Nitrogen
Sulphur

ABSTRACT

Volcanic emissions in shallow vents influence the biogeochemistry of the sedimentary compartment, creating marked abiotic gradients. We assessed the spatial dynamics of the sediment compartment, as for the composition and origin of organic matter and associated prokaryotic community, in a volcanic shallow $CO_2$ vent (Vulcano Island, Italy). Based on elemental (carbon, nitrogen content and their ratio) and isotopic composition ($\delta^{13}C$, $\delta^{15}N$ and $\delta^{34}S$), the contribution of vent-derived organic matter (microbial mats) to sedimentary organic matter was high close to the vent, while the marine-derived end-members (seagrasses) contributed highly at increasing distance. Chemoautotrophic *Campylobacterota* and hyperthermophilic *Achaea* prevailed close to the vent, whilst phototrophic and chemoheterotrophic members dominated at increasing distance. Abiotic gradients generated by the volcanic $CO_2$ vent drive relevant changes in the composition, origin and nutritional quality of sedimentary organic matter, and influence the structure and complexity of associated prokaryotic communities, with expected relevant impact on the entire food-web.

## 1. Introduction

Submarine volcanic vents occur worldwide in a variety of tectonic settings, from shallow to deep-sea (Rona and Scott, 1993; Price and Giovannelli, 2017). Particularly, shallow vents, frequently associated with coastal volcanism, are marked by high $pCO_2$, low pH and Eh values leading to acidic and reducing conditions, and often also by measurable concentrations of trace element (Dando et al., 1999; Vizzini et al., 2013). All these factors modify the abiotic support system of marine communities, influencing in different ways the structure, function, evolution and biogeographic history of these ecosystems (Tarasov et al., 2005). As naturally $CO_2$-enriched ecosystems, shallow volcanic vents have gained increasing attention as they may serve as analogues for future high $pCO_2$/low pH scenarios, acting as natural laboratories wherein to study *in situ* the effects of ocean acidification on biological and ecological features of coastal ecosystems, and to make predictions for future settings (Hall-Spencer et al., 2008). Currently, ocean acidification is an emergent global problem as a decrease by 0.3–0.4 pH units is predicted for the end of the current century (Hoegh-Guldberg et al., 2015; Orr et al., 2005) with severe effects on marine organisms and communities (Mostofa et al., 2015; Ullah et al., 2018; Vizzini et al., 2017).

The Aeolian Archipelago (Tyrrhenian Sea, Italy), consisting of seven main islands, hosts numerous shallow vents related to both active and extinct volcanism. Submarine vents release both thermal waters (27 - 130 °C) and gases, consisting mostly of $CO_2$ plus variable concentrations of reactive ($H_2S$, $O_2$, $CH_4$, CO and $H_2$) and inert ($N_2$, Ar and He) gases (Italiano and Nuccio, 1991; Sieland et al., 2009; Steinbrückner, 2009). Elemental sulphur, varying in colour from white to yellow-orange, is often found in sediments around the vents. Due to the spatio-temporal instability of volcanic inputs, seawater features generally undergo

---

* Corresponding author at: Department of Earth and Marine Sciences, University of Palermo, via Archirafi 18, 90123 Palermo, Italy.
*E-mail address:* giovanna.cilluffo@unipa.it (G. Cilluffo).

[1] These authors contributed equally

https://doi.org/10.1016/j.marpolbul.2024.117470
Received 10 October 2024; Received in revised form 10 December 2024; Accepted 15 December 2024
Available online 21 December 2024
0025-326X/© 2024 The Authors. Published by Elsevier Ltd. This is an open access article under the CC BY-NC-ND license (http://creativecommons.org/licenses/by-nc-nd/4.0/).

intrinsic small-scale variability (Boatta et al., 2013) with unstable gradients of gases and nutrients (*e.g.*, DIC and DIN; Capaccioni et al., 2001), which may be exacerbated or hampered by hydrodynamic and local meteorological conditions, overall generating environmental unpredictability and biological stochasticity.

Variability of volcanic inputs and their associated gradients may influence organic matter production, affecting the availability and nutritional quality of primary producers (Vizzini et al., 2017; Martínez-Crego et al., 2020). Several studies demonstrated that shift and substitution in macroalgae species occur, and seagrass biomass and density change along pH gradients, although with contrasting results (Arnold et al., 2012; Baggini et al., 2014; Hall-Spencer et al., 2008; Porzio et al., 2011; Vizzini et al., 2019). Origin of nutrients used by macrophytes was related in some cases to volcanic input (Apostolaki et al., 2014; Vizzini et al., 2010; Noè et al., 2020). Variation of organic matter typology, abundance and quality in $CO_2$ vents is expected to affect the upper trophic levels, but also detritus repository compartments, such as sediment. So far, however, little attention has been focused on the origin and dynamics of sedimentary organic matter (SOM) pool in $CO_2$ vents, although their features are expected to directly influence not only biogeochemical cycles, but also potentially the entire food web through bottom-up processes. Being a sink compartment, sediment receives organic matter of mixed origin (*e.g.*, micro- and macroalgae, seagrasses, autochthonous and allochthonous detritus). Moreover, in $CO_2$ vents, due to different sets of nutrients (of volcanic and marine origin) on which organic production may be based on, and to the peculiar environmental features (volcanic input; low pH and Eh values), the presence of additional sources of organic production (*e.g.*, photosynthetic and chemosynthetic microorganisms) may complex the SOM pool and consequently the ecosystem trophic structure (De Leeuw et al., 1995; Vizzini et al., 2017). Indeed, prokaryotes are able to tolerate both strong physical and chemical gradients generated from the vents. *Archaea* and *Bacteria* are the key drivers in the functioning of these ecosystems since they are involved in the transformation of inorganic compounds released from the vent emissions and are at the basis of the food web (Gugliandolo and Maugeri, 2019). Due to the shallow depths, both light and hydrothermal energy support a complex microbial community (Tarasov, 2006), displaying the presence of oxygenic and anoxygenic phototrophs (Giovannelli et al., 2013; Hirayama et al., 2007; Lentini et al., 2014; Maugeri et al., 2013), chemolithotrophs (Giovannelli et al., 2013; Gugliandolo et al., 2015), aerobic and anaerobic heterotrophs (Gugliandolo and Maugeri, 1998; Gugliandolo et al., 2012). Despite the success in culturing heat-loving *Archaea* and *Bacteria* from Aeolian vents, and especially from those in the Levante Bay of Vulcano Island (see for reviews Maugeri et al., 2010; Price and Giovannelli, 2017), most of the microbial diversity at shallow hydrothermal systems is still known only as gene sequences retrieved by molecular surveys (Gugliandolo and Maugeri, 2019).

In this study, the dynamics of SOM was analysed at a small spatial scale in a shallow area affected by volcanic emissions in relation to the changes in the photosynthetic and chemosynthetic community composition. The specific aims were: i) to discern the origin of SOM and the contribution of vent *vs.* marine end-members (respectively, the suspended particulate organic matter – SPOM – and the microbial mats from the primary vent *vs* the seagrasses and SPOM from the Control site); ii) to explore the influence of the vent input on photosynthetic and chemosynthetic communities associated with sediments, and iii) to identify the spatial extent of the area affected by $CO_2$ vent emissions with implications for ocean acidification studies.

## 2. Materials and methods

### 2.1. Study area

Levante Bay is a shallow bay located in the eastern side of Vulcano Island (Aeolian Archipelago, Italy, Tyrrhenian Sea) (Fig. 1), where emissions of volcanic fluids and gases are easily visible at the surface.

Diffuse submarine seepages in the form of dispersed underwater leaks occur, among which one of the most active bubbling, hereafter called primary vent (PV), is located at 38°25.057′N-14°57.599′E. The input consists mostly in $CO_2$ (97–99 % vol) and minor amounts of $H_2S$ (< 2.2 %), undetectable at a distance of about 150 m from the PV (Boatta et al., 2013; Capaccioni et al., 2001). $CO_2$, pH and carbonate saturation index gradients along the northern shoreline of the bay range between 76.2 and 99.1 %, 6.40 and 8.16, 0.03 and 5.63, respectively (Boatta et al., 2013; Vizzini et al., 2013). Details of measured seawater variables, temperature, pH, dissolved oxygen concentration (DO) and electrical conductivity of bottom water (Eh) are reported in Vizzini et al. (2013)

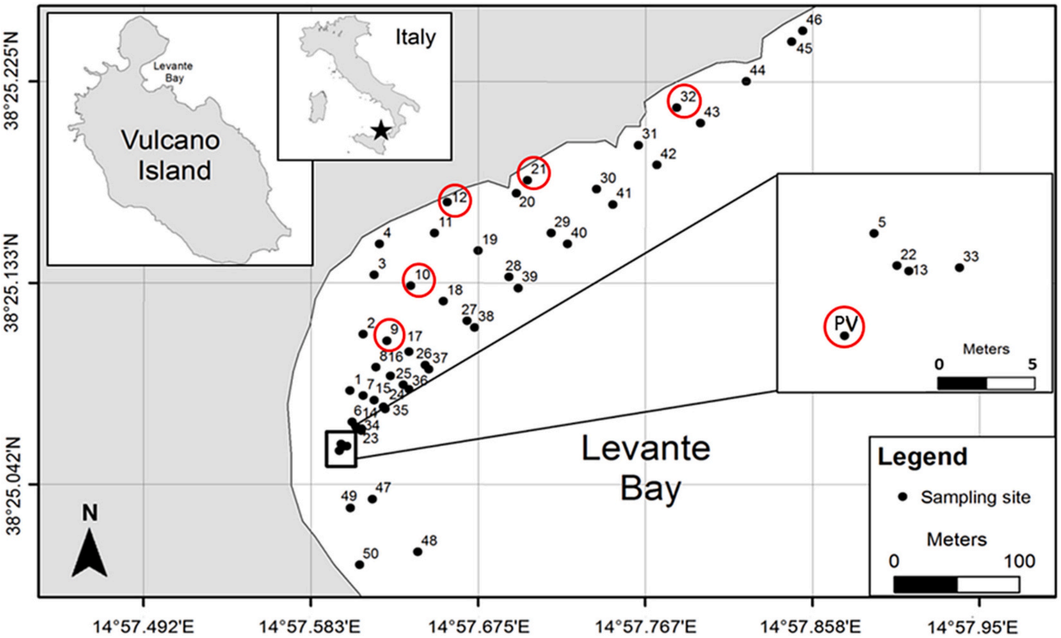

**Fig. 1.** Map of Levante Bay with sampling stations selected at increasing distance from the primary vent (PV). Sampling stations examined for microbial community diversity are indicated with red circles. (For interpretation of the references to colour in this figure legend, the reader is referred to the web version of this article.)

and confirm the pH/Eh gradient previously reported by Boatta et al. (2013). Sediments were overall sandy with low silt (mean ± s.d. = 1.1 ± 1.3 %) and organic matter content (1.3 ± 0.7 %) (Vizzini et al., 2013). OM content showed also a slightly decreasing pattern at increasing distance from PV (up to 150 m from PV: range 0.7 - 3.9 %, mean ± s.d. 1.7 ± 0.7 %; from 150 to 500 m from PV: 0.5 - 1.9 %, 0.8 ± 0.3 %) (Vizzini et al., 2013). The seabed was characterized by bare sediment around the PV and for approximately 220 m, after which macrophyte coverage occurred with patchy distribution of the seagrass species *Cymodocea nodosa*, interspersed with sparse macroalgae species, such as *Caulerpa prolifera, Cystoseira compressa* and *Dictyota dichotoma* occurring with low abundances (Vizzini et al., 2013, 2017).

### 2.2. Sample collection

Sampling was carried out in the central part of Levante Bay. Main physico-chemical variables of surface water (temperature, dissolved oxygen, pH and Eh) were recorded contextually to sediment collection using a multiparameter probe (Hydrolab DS5). Sediment samples were manually collected in duplicate by SCUBA divers, using PVC hand-cores (Ø 4 cm), from 47 stations distributed along five submarine transects that extend from PV up to a distance of ~500 m (Fig. 1) and a depth range between 0.7 and 5.5 m. The first 2-cm layer of each core was immediately sliced with a ceramic knife for subsequent analyses. Subsamples for organic matter analysis were collected from each core and stored at -20 °C until further processing. At six stations (Fig. 1), which were selected along an increasing pH gradient, sediment subsamples were also collected for microbial abundance estimation and DNA extraction; the formers were fixed with formaldehyde 2 % (*v*/v, final concentration), whereas the latter were directly stored at -20 °C until further processing.

PV and control site-specific sources of organic matter were collected as end-members, given their potential contribution to the SOM pool. Specifically, microbial mats were collected at the PV, as a volcanic vent end-member, by scraping the top layer of the mat-covered rocks with a ceramic knife, while macrophytes were collected as marine end-members, from the Control site located approximately 500 m from PV, which lacks evidence of gas venting (mean pH 8.2). Marine end-members were the seagrasses *Cymodocea nodosa* and *Zostera noltei*, that were collected manually by SCUBA divers and stored at –20 °C until analysis. No macrophytes samples were collected from the acidified site (PV) due to their negligible abundance, and hence contribution to the SOM. To analyse the SPOM from PV (SPOM-L) and the Control site (SPOM-C), seawater samples (10 l each) were collected in triplicate at these two sites using glass bottles.

### 2.3. Samples processing, element and stable-isotope analysis

Water samples were filtered through pre-combusted (450 °C, 4 h) Whatman GF/F filters and subsequently freeze-dried and ground into a fine powder using a micro-mill prior to analyses, along with sediment, microbial mats and seagrass samples. Sediment and organic matter sources (microbial mats, seagrasses and SPOM) were analysed for organic carbon ($C_{org}$, %), total nitrogen ($N_T$, %) and carbon and nitrogen stable isotopes ($\delta^{13}C$ and $\delta^{15}N$, ‰). Sulphur stable isotopes ($\delta^{34}S$, ‰) were analysed only in sediment samples. Samples for $C_{org}$ and $\delta^{13}C$ analysis were treated with HCl (5 N and 2 N, respectively) to remove carbonates. Powdered samples were weighed in silver (for $C_{org}$ analysis) and tin capsules (for $N_T$, $\delta^{13}C$ and $\delta^{15}N$ analysis). $C_{org}$ and $N_T$ were analysed using an elemental analyser (ThermoElectron Flash EA 1112), which was interfaced to an isotope ratio mass spectrometer (ThermoElectron Delta Plus XP) for the analysis of $\delta^{13}C$ and $\delta^{15}N$. Isotope values are given in the conventional δ notation as ‰ deviation from the standards (Vienna Pee Dee Belemnite for $\delta^{13}C$, atmospheric $N_2$ for $\delta^{15}N$, Vienna Canyon Diablo Troilite for $\delta^{34}S$) as follows: $\delta^{13}C$, $\delta^{15}N$ or $\delta^{34}S = [(R_{sample}/R_{standard}) - 1] \times 1000$, where R is the corresponding $^{13}C/^{12}C$, $^{15}N/^{14}N$ or $^{34}S/^{32}S$ ratio. The analytical precision of the measurements based on the standard deviation of replicates of internal standards (International Atomic Energy Agency IAEA-CH-6 for $\delta^{13}C$, IAEA-NO-3 for $\delta^{15}N$ and IAEA-S1 for $\delta^{34}S$) was 0.1 ‰ for $\delta^{13}C$ and 0.2 ‰ for $\delta^{15}N$ and $\delta^{34}S$. The detection limits of the elemental analyser used were respectively 0.01 % for $C_{org}$ and 0.005 % for $N_T$.

### 2.4. Analysis of prokaryotic communities

#### 2.4.1. Prokaryotic abundance

To detach cells from sediments, 1 g of each sample was diluted (1:10 weight/vol) in sterilized phosphate buffer solution (PBS, pH 7.4) containing sodium pyrophosphate (0.1 % vol/vol). Samples were sonicated for 10 cycles of 30 s using a Brandlin SonoPlus HD 200 (Electronic, Berlin). Cells were finally concentrated onto black polycarbonate membrane filters (0.2 μm pore size, 25 mm diameter, Nuclepore Corporation, Pleasanton, USA). To evaluate the abundance of total prokaryotic cells (total counts, TC), harvested cells were stained with 4',6-diamidino-2-phenylindole (DAPI) fluorochrome (1 μg $ml^{-1}$, final concentration) and counted by epifluorescence microscopy (Olympus BX-60 M, at 1000× magnification) under ultraviolet light (HG 100 W).

Fluorescence *in situ* hybridization (FISH) was employed to enumerate *Bacteria* and *Archaea* using rRNA-targeted oligonucleotide probes, according to Pernthaler et al. (2001). Cyanine-labeled (Cy3) probes EUB338 and ARCH915 (Thermo Hybaid, Interactiva Division, Ulm, Germany) were used to hybridize bacterial and archaeal cells, respectively. For each sample, between 50 and 200 cells were then counted under epifluorescence, using Olympus BX60 microscope, equipped with Cy3 filter set.

#### 2.4.2. Prokaryotic community composition evaluated by PCR- DGGE

DNA was extracted directly from sediment samples (1 g) using the PowerSoil DNA isolation kit (MoBio Laboratories, Carlsbad, CA, USA) according to the manufacturer's instructions. DNA concentrations and purity were checked by UV–Vis spectrophotometry (NanoDrop ND-1000Technologies, USA).

The V3 region of bacterial 16S rRNA gene was amplified with universal primer set 341f-GCclamp (5'-CCTACGGGAGGCAGCAG-3') and 907r (5'- CCGTCAATTCMTTTRAGTTT-3'), whilst the V3 region of *Archaea* 16S rRNA gene was amplified with primers ARC344f-GC (5'-ACGGGGTGCAGGCGCGA-3') and ARC915r (5'-GTGCTCCCCCG CCAATTCCT-3'). Bacterial and archaeal PCR products were resolved in polyacrylamide gels as described previously by Muyzer et al. (1996) and Casamayor et al. (2000) using a DGGE-2001 system (CBS Scientific Company, CA, USA). The most representative bands in DGGE gels were excised and placed in 50 μl of TE buffer 1× (10 mM Tris-HCl containing 1 mM EDTA $Na_2$, pH 8), incubated at 65 °C for 3 h to allow diffusion of DNA out the gel blocks. Each eluate was briefly vortexed one time for each hour, centrifuged at 10000 rpm for 5 min, and finally used as template DNA in PCR reamplification, with primers and conditions as described above.

Sequencing of DNA extracted from DGGE bands was performed with primers 341f for *Bacteria* and ARC344f for *Archaea* (Macrogen Inc., Seoul, Korea). A nucleotide BLAST search (http://www.ncbi.nlm.nih.gov/BLAST) was performed to obtain information on sequences from phylogenetically closest relatives. Phylogenetic trees were constructed using the MEGA 7 (Molecular Evolutionary Genetics Analysis) software. The robustness of the inferred trees was evaluated by 500 bootstrap resamplings. Bacterial phylogeny tree was out grouped with 16S rRNA gene sequence of *Methanocaldococcus jannaschii*, while that of archaeal phylogeny was out grouped with 16S rRNA gene sequence of *Cytophaga aurantiaca*.

### 2.5. Data analysis

Pearson's correlation analysis was used to assess the relationship between the SOM variables ($C_{org}$, $N_T$, $C_{org}$:$N_T$, $\delta^{13}C$, $\delta^{15}N$ and $\delta^{34}S$), and physico-chemical data of surface water (temperature, dissolved oxygen, pH and Eh). Maps of the spatial variability of $\delta^{13}C$, $\delta^{15}N$, $\delta^{34}S$ and $C_{org}$:$N_T$ in the SOM were created using QGIS 3.38. $\delta^{13}C$ and $\delta^{15}N$ data were used to estimate the proportional contribution of vent and marine organic matter sources to the SOM pool, using a Bayesian Mixing Model run through the MixSiar package v 3.1.12 (Stock and Semmens, 2013; Stock et al., 2018) in R v4.3.2 (R Core Team, 2018). Microbial mats and SPOM-L were regarded as vent sources, seagrasses and SPOM-C were regarded as marine sources. Distance from the vent was included in the model as explanatory variable and fractionation value of each source was set to zero as no trophic fractionation is expected to occur. In this framework, MixSiar estimates the probability contribution of each source to the SOM mixture. The Gelman diagnostic test was used to determine the convergence of the model (Stock and Semmens, 2013). The estimated mean contributions of marine and vent sources were summed *a posteriori* to simplify the graphical output. In addition, linear regression was performed using the mean contributions of marine and vent sources as response variables *vs.* the interaction between distance and the source (vent or marine).

DGGE band position and intensity were determined using a GELCOMPAR II software package (Applied Maths) and were manually modified. To compare community profiles among samples, Sorensen similarity coefficient ($S_s$) was applied to the banding patterns, and cluster diagrams were obtained using PRIMER 6.1.12 (Primer-E, Ltd). The total number of bands in each line was expressed as phylotype richness (*R*). The relative intensity was used to calculate the Shannon diversity (*H'*) and the evenness (*E*) indices, in order to describe possible changes in the DGGE profiles.

Pearson's correlation analysis was applied to determine the links between prokaryotic abundances (*Bacteria* and *Archaea*), diversity indices (*R*, *H'* and *E*), and the relative abundance of the dominant bacterial and archaeal groups, as derived by DGGE analysis, with the environmental variables retrieved from seawater (pH, OM%, taken from Vizzini et al., 2013) and sediment samples ($C_{org}$ and $N_T$). Principal Component Analyses (PCAs), based on selected properties of sediment samples (pH, OM%, $C_{org}$% and $N_T$%), prokaryotic cells abundance (TC) and diversity indices (*H'*, *E'* and *R*), was performed to identify groups of stations with similar community composition and to find their relationships with the environmental variables, by using PRIMER 6.1.12 (Plymouth Marine Laboratory, UK). Natural logarithm was used to equalize variances and normalize the data prior to these analyses.

## 3. Results

### 3.1. Element and stable isotope data

#### 3.1.1. Sedimentary organic matter (SOM)

Sedimentary organic carbon ($C_{org}$) and total nitrogen ($N_T$) were fairly low, ranging from 0.04 to 0.14 % (mean ± s.d.: 0.08 ± 0.02 %) and from 0.01 to 0.02 % (0.01 ± 0.00 %), respectively. The $C_{org}$:$N_T$ displayed spatial variations, ranging from 3.6 to 12.2 (6.7 ± 1.5) and showing progressively higher values at increasing distance from the primary vent (PV) (Fig. 2, 3).

$\delta^{13}C$, $\delta^{15}N$ and $\delta^{34}S$, varying respectively from −24.6 to −18.0 ‰ (−22.1 ± 1.5 ‰), from −5.1 to +3.8 ‰ (−1.2 ± 2.1 ‰) and from −1.4 to +16.2 ‰ (4.6 ± 4.9 ‰), exhibited a wide spatial variability and a clear enriching trend with increasing distance from PV (Fig. 2, 3).

Significant positive correlations among $\delta^{13}C$, $\delta^{15}N$ and $\delta^{34}S$ and physico-chemical variables of surface seawater (DO, Eh and pH: $p < 0.001$) were recorded (Fig. 4). In addition, $\delta^{13}C$, $\delta^{15}N$ and $\delta^{34}S$ were positively correlated each other ($p < 0.001$); $\delta^{13}C$ was positively correlated with $C_{org}$ ($r = 0.45$, $p < 0.001$) and $\delta^{15}N$ was negatively correlated with $N_T$ ($r = -0.33$, $p < 0.01$).

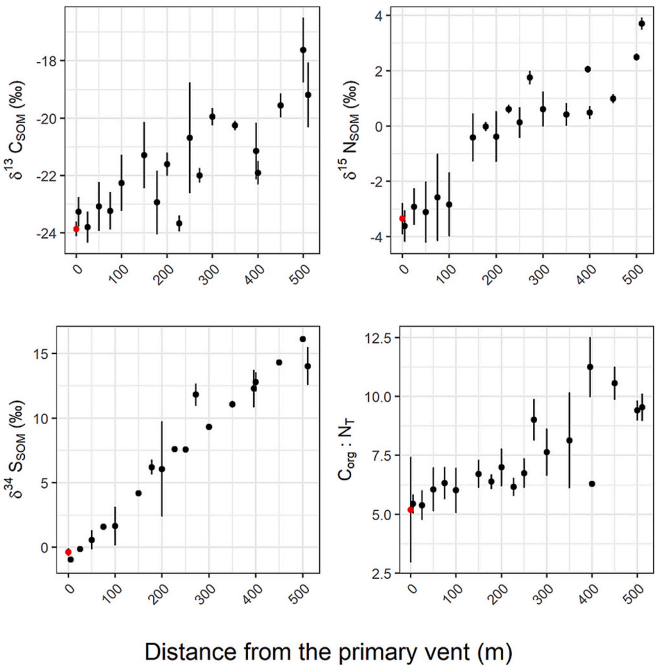

**Fig. 2.** $\delta^{13}C$ (‰), $\delta^{15}N$ (‰), $\delta^{34}S$ (‰) and $C_{org}$:$N_T$ ratio (mean ± s.d. of each station) in the sedimentary organic matter (SOM) from Levante Bay. SOM data from the primary vent are indicated with a red circle.

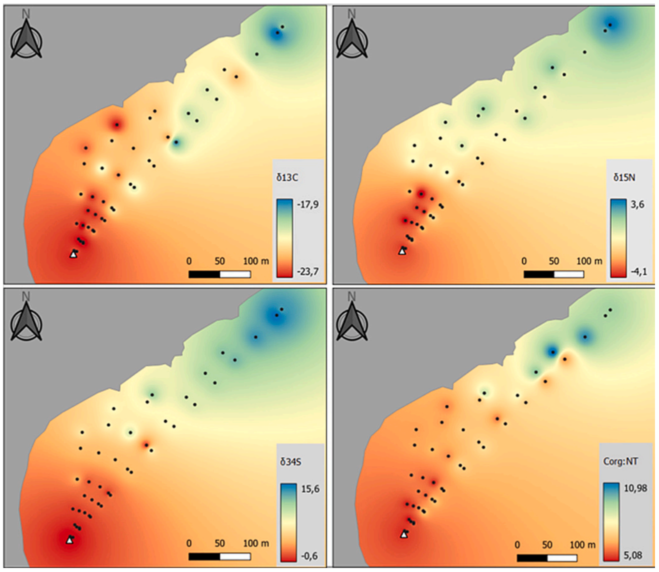

**Fig. 3.** Spatial variability of $\delta^{13}C$ (‰), $\delta^{15}N$ (‰), $\delta^{34}S$ (‰) and $C_{org}$:$N_T$ in the sedimentary organic matter (SOM) from Levante Bay. The primary vent station is indicated with a white triangle.

#### 3.1.2. Organic matter sources

Organic carbon ($C_{org}$) varied widely among the organic matter sources (from 0.6 to 35.6 %), while $N_T$ showed lower variability (from 0.1 to 1.7 %), with SPOM-C and seagrasses showing the lowest and the highest values for both variables (Fig. 5). SPOM-L also showed the lowest $C_{org}$:$N_T$ ratio, varying from 4.5 to 5.3, while seagrasses $C_{org}$:$N_T$ ratios showed the highest values, ranging between 18.1 and 24.7 (Fig. 5).

Organic matter sources showed distinct $\delta^{13}C$ and $\delta^{15}N$ values (Fig. 6). Specifically, $\delta^{13}C$ of SPOM-L showed fairly constant and $^{13}C$-depleted values, ranging from −24.9 to −24.6 ‰, while SPOM-C

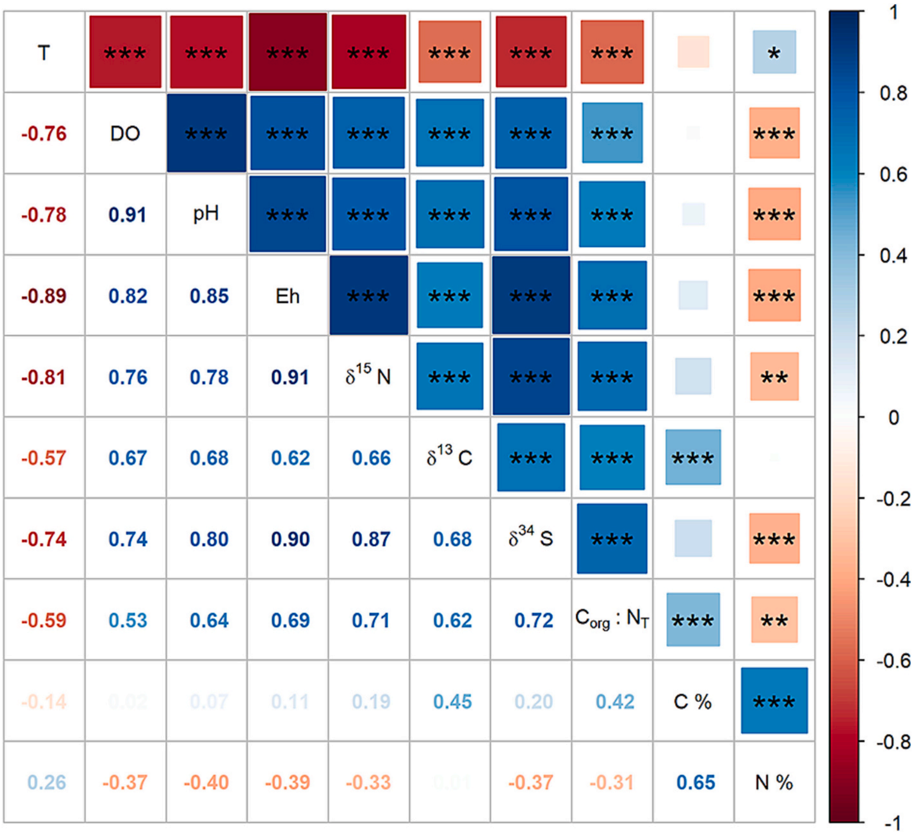

**Fig. 4.** Correlation plot: the upper panel reports the colour of correlations in square (darker square indicates higher correlation in absolute value), and the lower panel portrays the estimated coefficients. The square colour represents the direction of correlation (red = negative correlation, blue = positive correlation), stars represent the significant level of correlation coefficients. (For interpretation of the references to colour in this figure legend, the reader is referred to the web version of this article.)

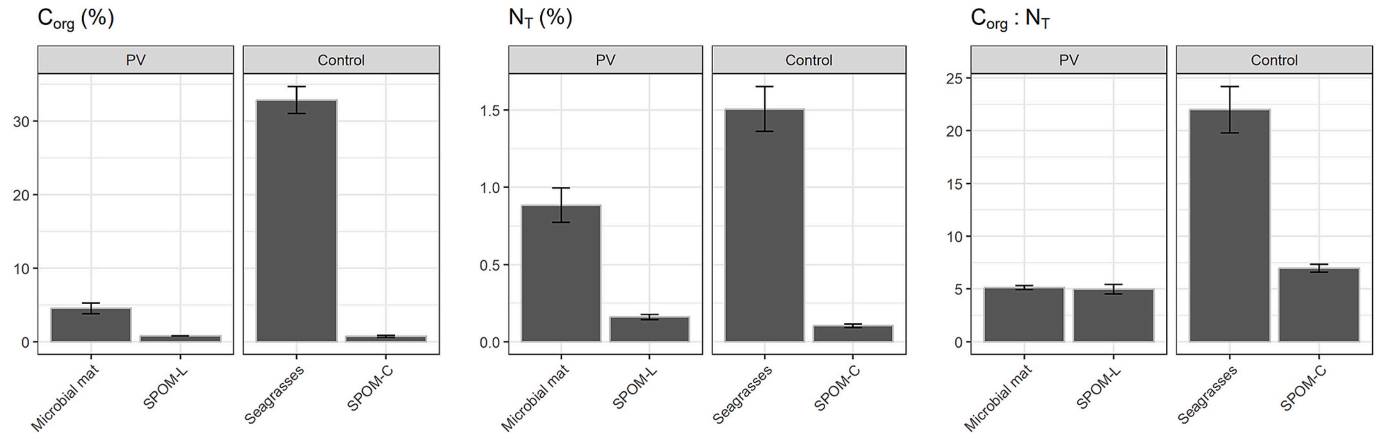

**Fig. 5.** $C_{org}$ (%), $N_T$ (%) and $C_{org}$:$N_T$ ratio (mean ± s.d.) in organic matter sources from the vent site at Levante Bay (microbial mats and SPOM-L) and the Control site (seagrasses and SPOM-C).

exhibited a slightly wider range and more $^{13}$C-enriched values, varying from −22.1 to −20.2 ‰. $\delta^{13}$C was widely variable and depleted in the microbial mats collected in PV (range from −27.4 to −18.9 ‰), while more enriched in seagrasses (from −13.0 to −7.8 ‰). In contrast, $\delta^{15}$N varied little within each source group. Microbial mats were the most $^{15}$N-depleted source (from −4.9 to −2.7 ‰). $\delta^{15}$N of seagrasses (from 0.7 to +2.1 ‰) was slightly more depleted than that of SPOM-L (from 1.2 to 2.2 ‰) and SPOM-C (from 3.7 to 4.9 ‰).

### 3.1.3. *MixSiar results*

MixSiar outcome revealed that the origin of organic matter in sediments was complex and the proportional contribution of each source varied with the distance from the primary vent (Table A1). A significant interaction was found between vent or marine source and distance from the vent. In particular, the effect on proportional contribution of the vent end-members decreased at increasing of the distance; on the contrary the effect on proportional contribution of the marine source increased at increasing of the distance (Fig. 7).

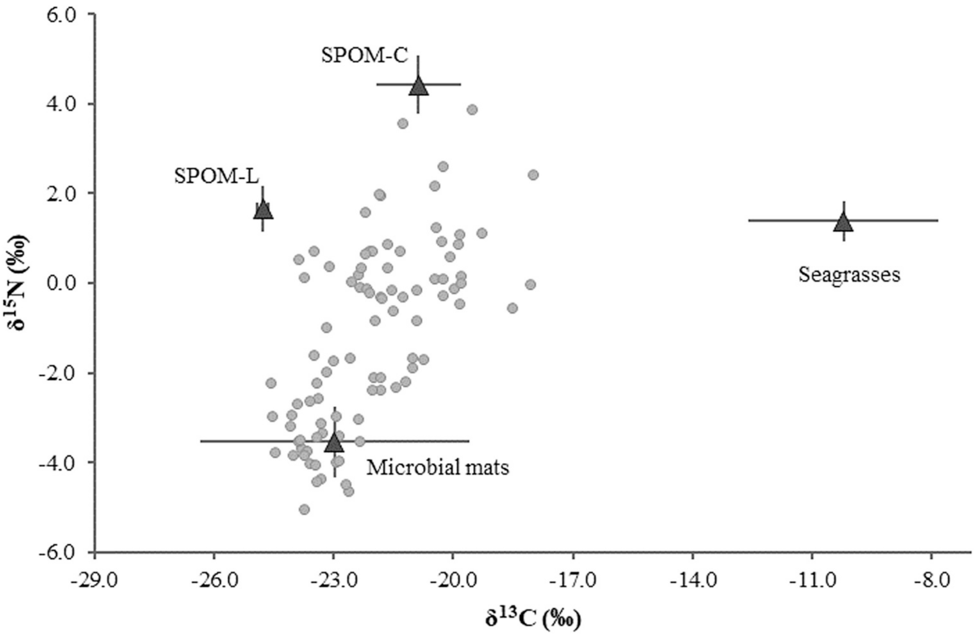

**Fig. 6.** $\delta^{13}C$ (‰) and $\delta^{15}N$ (‰) (mean ± s.d.) of organic matter sources in Levante Bay. SOM values are showed in grey.

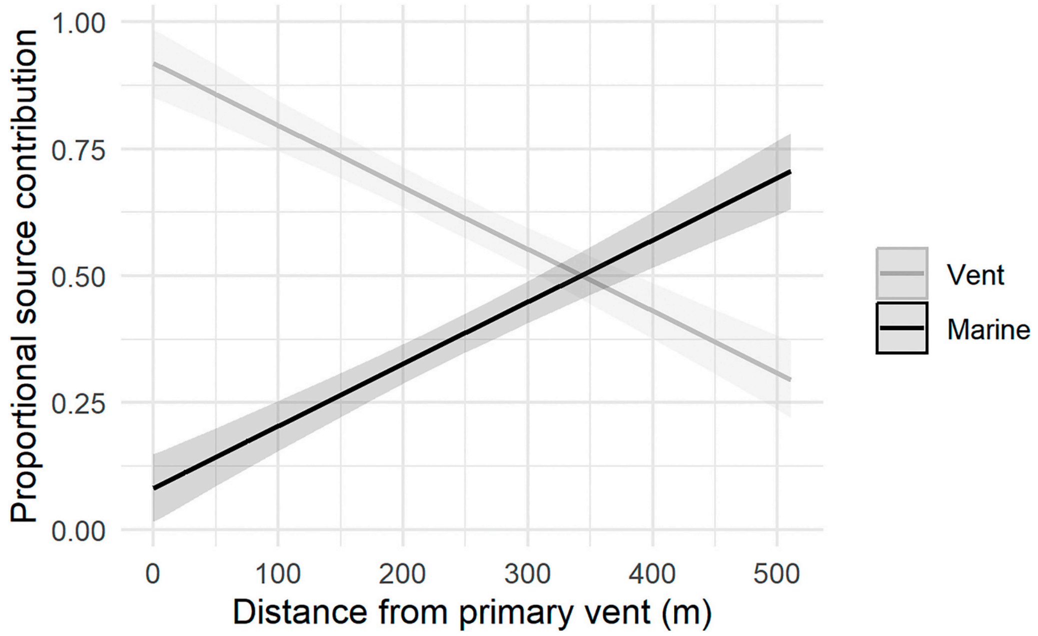

**Fig. 7.** Mean proportional contribution (± s.d.) of organic matter sources grouped as vent end-members (microbial mats and SPOM-L) and marine end-members (seagrasses and SPOM-C) to SOM at increasing distance from the primary vent, based on MixSiar output. Linear regressions are also shown, with the associated 95 % confidence interval.

### *3.2. Prokaryotic communities*

#### *3.2.1. Prokaryotic abundance*

Total prokaryotic cell counts (TC) obtained after DAPI staining, and abundance of hybridized cells with probes for *Bacteria* (EUB338) and *Archaea* (ARCH915) in sediment samples are reported in Table 1. *Bacteria* always numerically dominated over *Archaea*. Archaeal contribution (ranging from 0.1 to 1.1 %) was higher at PV.

#### *3.2.2. DGGE profiles*

The number and intensity of DGGE bands provided valuable information about variations in highly abundant operative taxonomic units,

**Table 1**
Total prokaryotic cell counts (TC) and abundances of hybridized cells with probes for *Bacteria* (EUB338) and *Archaea* (ARCH915) in sediment samples collected from the Levante Bay.

| Station | TC (cells g$^{-1}$) | *Bacteria* (%)[a] | *Archaea* (%)[a] |
|---|---|---|---|
| PV | $4.2 \times 10^6$ | $2.9 \times 10^6$ (98.9) | $3.2 \times 10^4$ (1.1) |
| 9 | $2.3 \times 10^7$ | $9.9 \times 10^6$ (99.8) | $1.5 \times 10^4$ (0.2) |
| 10 | $3.5 \times 10^7$ | $9.1 \times 10^6$ (99.7) | $2.9 \times 10^4$ (0.3) |
| 12 | $1.3 \times 10^7$ | $4.9 \times 10^6$ (99.3) | $3.3 \times 10^4$ (0.7) |
| 21 | $7.9 \times 10^6$ | $2.7 \times 10^6$ (99.9) | $3.7 \times 10^3$ (0.1) |
| 32 | $5.2 \times 10^6$ | $1.5 \times 10^6$ (99.6) | $6.5 \times 10^3$ (0.4) |

[a] In brackets, the percentage of cells recovered by FISH.

whose relative proportion is >1 % of the total microbial community (Muyzer et al., 1993). DGGE profiles and the analysis of *Bacteria* and *Archaea* community structure are reported in Fig. 8. The total number of bands (or phylotype richness) identified in each profile ranged from 10 (station 21) to 15 (station 9) for *Bacteria,* and from 6 (station 32) to 20 (stations PV, 10 and 12) for *Archaea* (Fig. 8a), suggesting a greater archaeal richness in the proximity of PV. Overall, *Bacteria* populations retrieved in sediment samples appeared more similar each other (60 % $S_s$) than those of *Archaea* (40 % $S_s$) (Fig. 8b). More similar bacterial populations were collected from stations 10 and 12, while those from PV were distantly related with those from the other stations. Archaeal populations from stations 9 and 10 were more similar each other, whereas those from PV and station 32 were clearly different from the others.

### 3.2.3. *Comparison between bacteria and archaea communities*

Both *Bacteria* and *Archaea* richness (*R*) and *H'* diversity indices, as derived by DGGE profiles, decreased by increasing distance from PV (Fig. 9).

The PCA for *Bacteria* showed that the two main components explained 78.6 % of the total variance (Fig. 10). The first principal component (Axis 1, explaining 62.1 % of the variance) was strongly associated with the organic matter content (OM%), pH, cell bacterial abundance (AB), richness (R) and diversity (H'). The second principal component (Axis 2, explaining 16.5 % of the variance) was mainly related to $C_{org}$%, $N_T$%, and *E'*. The combination of the two main components clearly separated stations PV and 32, whilst stations 12 and 21 remained closer and 9 and 10 clustered apart. PCA clusters appeared quite different to those resulted from DGGE profiles, indicating that a combination of environmental factors and sediment properties shaped the bacterial community diversity. Moreover, the Pearson's analysis showed that all environmental variables (*e.g.*, OM, $C_{org}$ and $N_T$) and diversity indices (*e.g.*, *R* and *H'*) were strongly negatively correlated ($p < 0.01$) with pH. Strong positive correlations ($p < 0.01$) were observed between $C_{org}$ and $N_T$ with bacterial *H'* and *R*. Furthermore, OM% showed a strong positive correlation ($p < 0.01$) with $C_{org}$, $N_T$ and *H'*.

The PCA for *Archaea* showed that the two main components of PCA explained 77.1 % of the total variance. The first principal component (Axis 1, explaining 47.7 % of the variance) was associated with pH, OM %, R and H' index, whilst the second principal component (Axis 2, 29.3 % of the variance) was strongly related to $C_{org}$ and E' index. The two main components clearly separated PV from the other stations, whilst clustered stations 9 and 10*,* confirming the results obtained by cluster analysis from the DGGE of *Archaea.* As expected, OM% and pH values were strongly and inversely correlated ($p < 0.01$).

### 3.2.4. *Phylogenetic analysis*

Excised DGGE bands and the level of 16S rRNA sequence identity to the most closely related cultivated strains of *Bacteria* and *Archaea* are reported in Table 2.

None of bacterial bands was unique to one sample, indicating that common phylotypes were present along the stations, even if different arrangements in bacterial aggregation were observed. Bands 1, 3 and 5 were common to all stations, band 6 was observed in all samples except for PV, and band 8 was common only to samples from PV and 32. Phylogenetic trees of the recovered bacterial and archaeal phylotypes are shown in Fig. 11.

Sequences of the dominant bacterial populations were related to the phyla *Campylobacterota* (bands 1 and 7)*, Bacteroidota* (bands 6 and 8) and *Cyanobacteriota* (bands 3, 4 and 5)*,* almost all already detected in hydrothermal systems or in other marine environments (Fig. 11a). Only band 2, common to stations PV and 32, was affiliated with *Actinomycetota,* genus *Acidimicrobium*. Band 1, related to *Sulfurovum*, was observed across all samples and was the most intense at PV, whereas band 7, related to *Sulfurospirillum,* was common to stations 9, 10 and 12. Bands 6 and 8 were related to two different genera within *Bacteroidota*: *i. e.*, *Maritimimonas*, and *Lewinella.* Sequences from bands 3 and 5, affiliated with *Cyanobacteriota* and related to the genus *Loriellopsis* and *Brasilonema*, respectively, were common to all samples, whereas sequences from band 4, related to the genus *Anabaena* were common to stations 9, 10 and 12.

Archaeal sequences were affiliated with the phyla *Euryarchaeota* and

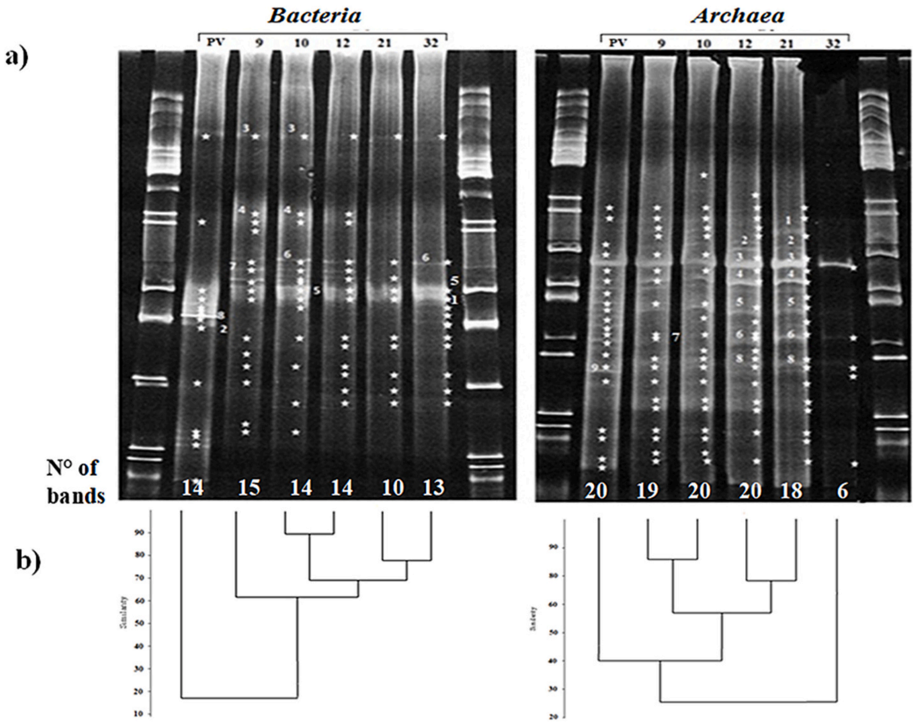

**Fig. 8.** DGGE profiles of *Bacteria* and *Archaea* obtained from sediment samples collected at increasing distance from the primary vent (PV) (a), and dendrograms representing *Bacteria* and *Archaea* community structure (b). Sequenced bands are indicated by numbers.

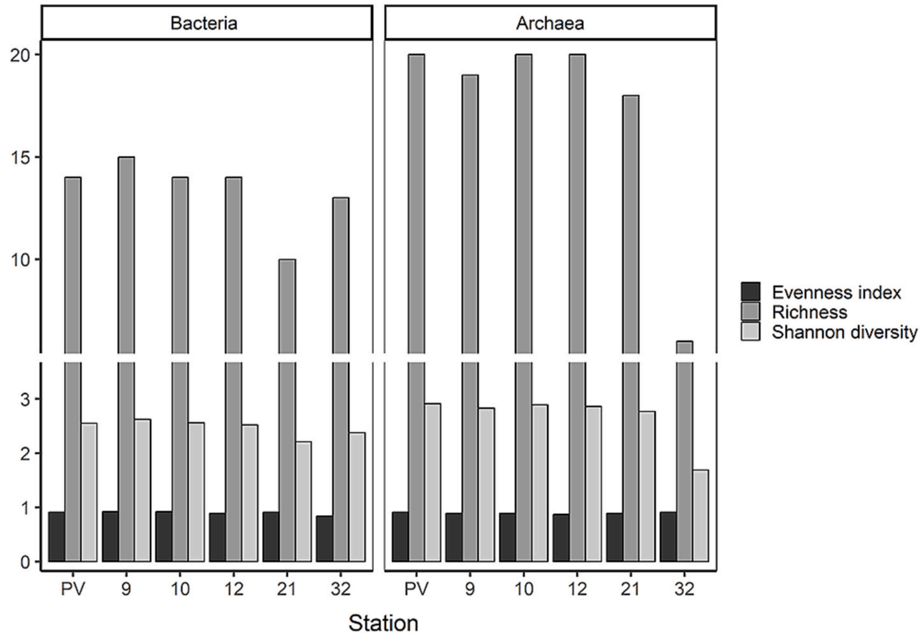

**Fig. 9.** Comparison of diversity indices (*H*', Shannon diversity; *E*', Evenness index, and *R*, Richness) of *Bacteria* and *Archaea* associated with sediments at increasing distance from the PV in Levante Bay.

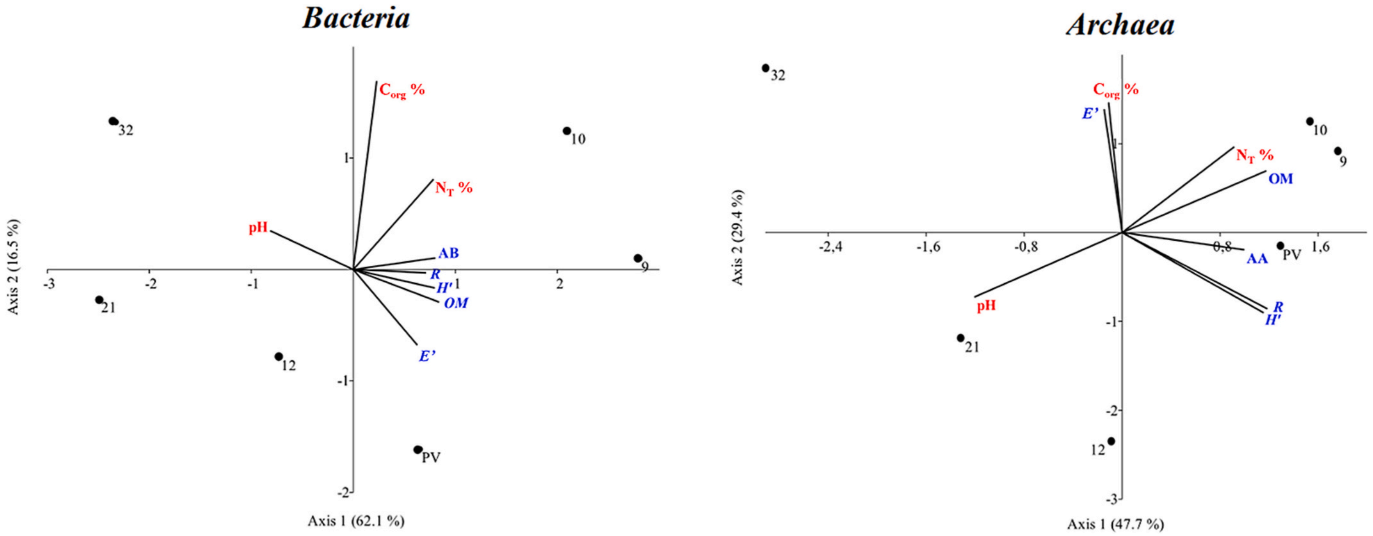

**Fig. 10.** Principal Component Analysis (PCAs) based on environmental data and prokaryotic properties for *Bacteria* and *Archaea* retrieved in sediment from the Levante Bay. OM%: organic matter content, $C_{org}$%: organic carbon content; $N_T$%: total nitrogen content. AB, hybridized *Bacteria*; AA, hybridized *Archaea*; *R*, richness; *H'*, Shannon diversity and *E'*, Evenness index.

*Thermoproteota*, and all phylotypes were related to *Archaea* retrieved from extreme environments, most of which characterized by high temperatures. Sequences from the most intense band 3, retrieved across all stations, and band 7, characteristic of station 32, fell into the class *Thermococci* and were related to the strictly anaerobic, hyperthermophilic genus *Thermococcus.* The phylotype from band 5 was related to the genus *Methanobrevibacter* (class *Methanobacteria*), which comprises mesophilic, strictly anaerobic, methanogens. Within the *Thermoproteota*, all sequences were related to different members of the class *Thermoprotei*. Phylotypes from bands 1, 4, and 6, retrieved in all stations with the only exception of station 32, were affiliated to the hyperthermophilic genera *Desulfurococcus*, *Vulcanisaeta* and *Stetteria,* respectively. Finally, bands 2 and 8 (common to stations 9, 10, 12 and 21) were affiliated with the hyperthermophilic genera *Thermogladius* and *Pyrolobus*, respectively.

## 4. Discussion

Pronounced spatial variations and gradients based on the distance from a shallow $CO_2$ vent were detected in SOM composition and origin, and in complexity of associated communities, highlighting a clear influence of volcanic emissions on biogeochemical features of the area in proximity of the vent.

The assessment of the contribution of the potential organic matter sources to the sedimentary pool was allowed by the distinct elemental and isotopic signatures of the vent (*i.e.*, microbial mats and volcanic vent-derived particulate organic matter) and marine (*i.e.*, seagrasses and marine-derived particulate organic matter) end-members. Consistently

**Table 2**
Distribution of *Bacteria* and *Archaea* arranged by samples collected from Levante Bay, as elucidated by PCR/DGGE profiles.

| | Band | Samples where bands are present | BLASTn most related species | Percentage of identity | Phylogenetic affiliation | Accession no. |
|---|---|---|---|---|---|---|
| Bacteria | 1 | All | *Sulfurovum aggregans* Monchim 33 | 100 | Campylobacterota | NR_126188 |
| | 2 | PV and 32 | *Acidimicrobium ferrooxidans* KME24 | 100 | Actinomycetota | MT940853 |
| | 3 | All | *Loriellopsis cavernicola* LF-B5 | 100 | Cyanobacteriota | NR_117881 |
| | 4 | 9, 10 and 12 | *Anabaena cylindrica* FACHB1038 | 100 | Cyanobacteriota | KR813843 |
| | 5 | All | *Brasilonema angustatum* HA4187-MV1 | 100 | Cyanobacteriota | NR_125582 |
| | 6 | 9, 10, 12, 21 and 32 | *Maritimimonas rapanae* A31 | 93 | Bacteroidota | NR_116269 |
| | 7 | 9, 10 and 12 | *Sulfurospirillum multivorans* DSM 12446 | 100 | Campylobacterota | NR_121740 |
| | 8 | PV and 32 | *Lewinella cohaerens* ATCC 23123 | 100 | Bacteroidota | NR_115012 |
| Archaea | 1 | PV, 9, 10, 12 and 21 | *Desulfurococcus fermentans* DSM 16532 | 99 | Thermoproteota | NR_102931 |
| | 2 | 9, 10, 12 and 21 | *Thermogladius shockii* WB1 | 99 | Thermoproteota | NG_044969 |
| | 3 | All | *Thermococcus barossii* DSM 9535 | 98 | Euryarchaeota | NR_042735 |
| | 4 | PV, 9, 10, 12 and 21 | *Vulcanisaeta souniana* IC-059 | 99 | Thermoproteota | NR_028628 |
| | 5 | PV, 9, 10, 12 and 21 | *Methanobrevibacter filiformis* RFM-3 | 98 | Euryarchaeota | NR_044801 |
| | 6 | PV, 9, 10, 12 and 21 | *Stetteria hydrogenophila* 4ABC | 98 | Thermoproteota | NR_044913 |
| | 7 | 32 | *Thermococcus chitonophagus* DSM 10152 | 98 | Euryarchaeota | NR_042737 |
| | 8 | 9, 10, 12 and 21 | *Pyrolobus fumarii* 1 A | 97 | Thermoproteota | NR_102985 |

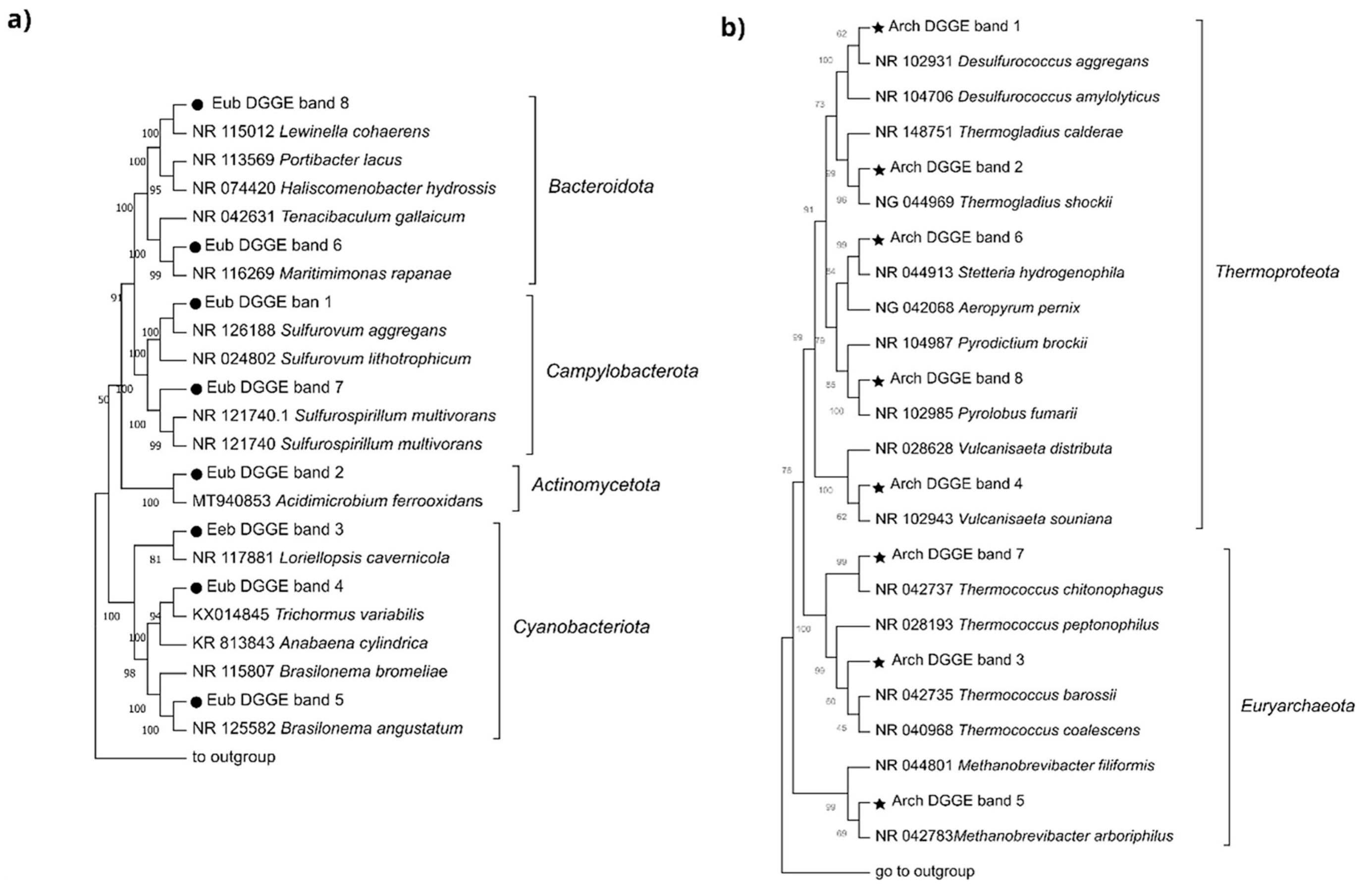

**Fig. 11.** Rooted phylogenetic trees calculated by Jukes-Cantor distance estimation algorithm showing affiliation of each DGGE-band to closest-related sequences from either cultivated or cloned *Bacteria* (a) and *Archaea* (b). Percentages of 1000 bootstrap resampling that supported the branching orders in each analysis are shown above or near the relevant nodes.

with De Leeuw et al. (1995) and Vizzini et al. (2017), microbial mats and SPOM from the primary vent were both characterized by a depletion in $^{13}$C, which can be easily associated with the influence of volcanic vent-derived dissolved inorganic carbon (unpublished data: DIC $\delta^{13}C = -1.9$ ‰). Vent-derived DIC is more $^{13}$C-depleted than marine-derived DIC (Papadimitriou et al., 2005), as it is almost exclusively composed of $CO_2$ (Vizzini et al., 2010). Therefore, autotrophic bacteria that characterise the bottom of the primary vent can synthesise new biomass with highly depleted carbon isotopic values, not only due to their reliance on the available $^{13}$C-depleted $CO_2$ but also due to the kinetic fractionation of carbon isotopes associated with the metabolic and biosynthetic processes (Gong and Hollander, 1997). In addition, values of SPOM, consisting of phytoplankton and fragments of microbial mats torn off from the rocks by the turbulent venting activity, mirrored the carbon isotopic signature of the microbial mats, resulting in much more $^{13}$C-depletion than its marine counterpart. Microbial mats from the primary vent were also very $^{15}$N-depleted. Although data from Levante Bay are unavailable, volcanic vents are known to release N in various forms (Dando et al., 1999; Maugeri et al., 2009; Tarasov et al., 2005). To our knowledge, the isotopic composition of DIN has never been investigated but, based on the lower $\delta^{15}N$ values of SPOM at the vent than at the control found in this study, and confirmed by the low $\delta^{15}N$ of macrophytes close to volcanic $CO_2$ vents (Apostolaki et al., 2014; Ricevuto et al., 2015; Vizzini et al., 2017), it is supposed to be more depleted than marine DIN.

By contrast, marine-derived organic matter sources (seagrasses and SPOM) showed more $^{13}C$-and $^{15}N$-enriched isotopic values than volcanic vent-derived ones, since the marine dissolved inorganic C and N pools are more enriched than the volcanic ones (marine DIC $\delta^{13}C = 0 \pm 1$ ‰, Papadimitriou et al., 2005; marine DIN $\delta^{15}N = 0 - +1, +2 - +19$ and $-3.5 - +7.5$ ‰ for $N_2$, $NO_3^-$ and $NH_4^+$ respectively; *e.g.*, Altabet, 2006; Brandes and Devol, 1997; Karl et al., 2002). $\delta^{13}C$ and $\delta^{15}N$ values found here match closely those reported in the literature for other marine coastal ecosystems (seagrasses: $\delta^{13}C = -15$ to $-3$ ‰, Michener and Kaufman, 2007, $\delta^{15}N = 0$ to $+8$ ‰, Lepoint et al., 2004; SPOM, used here as a proxy for phytoplankton: $\delta^{13}C = -22$ to $-20$ ‰, Meyers, 1997, $\delta^{15}N = +2$ to 8 ‰, Signa et al., 2012).

The isotopic values of sediments encompassed those of both vent and marine end-members, except for seagrasses that were more $^{13}C$-enriched, indicating that both vent and marine end-members contribute to the SOM pool. In more detail, SOM $\delta^{13}C$ and $\delta^{15}N$ displayed the most depleted values close to the primary vent, suggesting a high contribution of vent end-members, while they increased almost linearly with distance. This trend was more evident for $\delta^{15}N$ than for $\delta^{13}C$, whose increment was clear up to about 350 m from the primary vent. When moving far away from the vent, the overall enrichment in heavy isotopes suggests a decline in the contribution of volcanic vent-derived sources and, conversely, an increase in that of marine sources (*i.e.*, seagrasses and SPOM-C) to SOM pool. Close to the primary vent, volcanic vent end-members showed an overall proportional contribution of about 80 %, with microbial mats that colonise the seabed having the role of the main contributor. This result confirms the important direct influence of volcanic activity on the organic matter pool. At increasing distance from the vent, microbial mats and SPOM-L contribution decreased, while the proportion of seagrasses and especially SPOM-C to the SOM pool greatly increased. At 350 m from the primary vent, the role of volcanic vent-derived organic matter became less relevant with an overall proportional contribution of about 50 %. However, volcanic vent-derived organic matter was detected in sediments all over the bay, even at the distance of 500 m from the primary vent, and with proportions of about 40 % up to 400 m. This result testifies a wide-scale effect of the vent on the biogeochemistry of the area and specifically on the origin of SOM.

Sulphur isotopes, although analysed only in SOM and hence not included in the mixing models, provide further interesting insights, being a good indicator of the origin of organic matter (Peterson and Howarth, 1987). Similarly to $\delta^{13}C$ and $\delta^{15}N$, the spatial pattern of $\delta^{34}S$ along the bay showed a linear increase at increasing distance from the primary vent, due to the decreasing influence of volcanic input. Volcanic vent-derived organic matter is expected to be $^{34}S$-depleted, as sedimentary sulphide species, easily detectable in reducing environments, usually display low $\delta^{34}S$ values (from $-20$ ‰ to $-10$ ‰; Strauss, 1997). Here, there was no clear isotopic evidence for *in situ* $H_2S$ production by microbial sulphate reduction, which would have typically shown very $^{34}S$-depleted values (Böttcher et al., 2004). This suggests that, presumably, biogenic $H_2S$ generation (*i.e.* by sulphate reducing bacteria) is a minor process relative to the dominant advective (abiotic) $H_2S$ flux emitted from the $CO_2$ primary vent. Accordingly, the seafloor around the vent hosts an active microbial community, mainly composed by chemolithotrophic sulphide oxidizing bacteria (Gugliandolo and Maugeri, 1993). On the other hand, at increasing distance from the primary vent, SOM was mainly affected by marine end-members (seagrasses and SPOM) that generally exhibit a $\delta^{34}S$ range between $+15$ and $+ 21$ ‰ (Peterson and Fry, 1987), matching the sulphur isotope composition of sulphate in seawater ($\sim +21$ ‰; Rees et al., 1978). Therefore, the $\delta^{34}S$ variability observed in Levante Bay depends on the different influence of volcanic input along the spatial gradient.

This picture about the origin of SOM is confirmed by the spatial pattern of SOM $C_{org}$:$N_T$ ratio. The progressive increase of the $C_{org}$:$N_T$ ratio at increasing distance from the primary vent suggests a gradual reduction in the contribution of more labile organic matter sources (*e.g.*, microbial mats) alongside an increase in more refractory ones (*e.g.*, seagrasses). The low SOM $C_{org}$:$N_T$ ratio close to the primary vent indicated that sedimentary carbon derives largely from the *in situ* production (*i.e.*, microbial mats and SPOM-L) rather than through heterotrophic carbon influx and processing. Furthermore, this labile organic matter offers a unique habitat for autotrophic and heterotrophic microorganisms, constituting a significant carbon source (Svensson et al., 2004). Indeed, microbial mats associated with submarine volcanic vents showed low $C_{org}$:$N_T$ ratios, consistent with previously reported values for bacteria from Vulcano Island vents ($C_{org}$:$N_T$ = 3.8–9.4, Gugliandolo and Maugeri, 1998) and elsewhere ($C_{org}$:$N_T$ = 2.8–14.3, Fagerbakke et al., 1996). At more distant stations, the higher $C_{org}$:$N_T$ ratio confirms that SOM was more influenced by more refractory organic matter sources, such as seagrasses, which had high $C_{org}$:$N_T$ ratios. This pattern matches the distribution of macrophytes, which were absent close to the primary vent up to a distance of around 220 m, where they start forming a low-density meadow, which become denser at greater distance. While high $CO_2$ levels are supposed to promote macrophyte production in volcanic vents, other environmental factors, such as $H_2S$, toxic trace elements and low pH conditions, may cover up this positive effect prompting, instead, poor environmental conditions unsuitable for many macrophyte species. This result opens a question about the theory that macrophytes and especially seagrasses may be "winners" in a high $CO_2$ world (Russell et al., 2013) as reducing conditions of acidified seawater mobilise trace elements (*e.g.*, As, Cd, Cu, Fe, Hg, Mn, Zn) (Tarasov et al., 2005), increasing their bioavailability with potential biological and ecological consequences.

The complex features of SOM and its origin are paralleled in the biocomplexity and structural shifts that occurred in the photosynthetic and chemosynthetic communities. Indeed, volcanic emissions had contrasting effects on the benthic prokaryotic communities, which resulted in different photosynthetic and chemosynthetic assemblages. Although the prokaryotic abundances remained quite constant in all samples, differences in both bacterial and archaeal composition were highlighted by PCR/DGGE, that is considered the most reliable tool to analyse the microbial community diversity of dominant phylotypes (≥1 % of the total microbial community).

While the abundance of *Archaea* was lower than that of *Bacteria*, in line with previous studies in volcanic vents of Aeolian Islands (Gugliandolo et al., 2015; Maugeri et al., 2010), a highly diverse archaeal community, principally composed of hyperthermophilic members within *Euryarchaeota* (*Thermococci*) and *Thermoproteota* (*Thermoprotei*), was detected in the proximity of the primary vent. This finding was in line with previous observations by Antranikian et al. (2017), who detected a high abundance of hyperthermophilic *Archaea* at shallow vents of Vulcano Island. Due to their pH dependence, *Thermoprotei* (*Desulfurococcus*, *Pyrolobus*, *Stetteria*, *Thermogladius* and *Vulcanisaeta*) are replaced by both *Thermococci* (*Thermococcus*) and *Methanobacteria* (*Methanobrevibacter*), determining a marked shift in the archaeal population composition at increasing distance from the primary vent.

Here, the bottom is featured by stones and rocks covered by whitish microbial mats consisting almost entirely of chemolithoautotrophic sulphur -oxidizing bacteria (*Campylobacterota*), whose growth is favoured by $H_2S$ input from the vent and negative Eh conditions (Gugliandolo et al., 2006; Vizzini et al., 2013). The lower $\delta^{34}S$ observed close to the primary vent suggests a sulphur utilisation by sulphur-oxidizing bacteria, whereas the higher $\delta^{34}S$ measured at increasing distance from the primary vent may reflect a greater input of marine-derived organic matter and/or the mixing with ambient seawater that prevents any signal from microbial sulphide oxidation. Sequences related to *Sulfurovum* dominated at PV, whereas those of *Sulfurospirillum* were retrieved at stations closer to PV (*e.g.,* 9, 10, and 12). Both genera are considered characteristic inhabitants in both shallow and deep-sea hydrothermal vents, distributed in modern and ancient systems all over the world, where they are involved in the carbon and sulphur biogeochemical cycles (Campbell et al., 2006; Giovannelli et al., 2013; Gugliandolo et al., 2015; Patwardhan et al., 2018; Vetriani et al., 2014). Differently from *Sulfurospirillum spp.*, *Sulfurovum spp.* require a very narrow range of redox conditions, characterized by high sulfide concentration, and therefore they occur as pioneer colonizers of biofilm communities in $H_2S$ -enriched hydrothermal vents (Inagaki et al., 2004; Patwardhan et al., 2018). Mesophilic sulphur-oxidizing bacteria represent a specialized community in this area, involved in the chemosynthetic primary production and the turnover of the reduced sulphur compounds. The lower $\delta^{34}$S observed close to the primary vent suggests a sulphur utilisation by sulphur-oxidizing bacteria (*Campylobacterota*), whereas the higher $\delta^{34}$S measured at increasing distance from the primary vent may reflect a greater input of marine-derived organic matter and/or the mixing with ambient seawater that prevents any signal from microbial sulphide oxidation.

Beneath microbial mats, a variety of microhabitats allows the autotrophic growth in low light environments, such as photosynthesizing *Cyanobacteriota* (*e.g.*, genera *Anabaena, Brasilonema*, and *Loriellopsis*) also involved in the nitrogen fixation. Therefore, their presence may explain the low $\delta^{15}$N values recorded at PV and the closest sites, as well as previously suggested in volcanic vents located in different geographical areas (Mehta and Baross, 2006).

At increasing distance from PV, mesophilic chemoheterotrophic members of *Bacteroidota* and *Actinomycetota* were dominant, that are known to be proficient in degrading various complex biopolymers, such as cellulose, chitin and pectin (Kirchman, 2002), derived from eukaryotic organisms.

A spatial pattern was also recorded for macrophytes: while whitish microbial mats feature the rocky bottom at the primary vent, at increasing distance from the vent, the sediment becomes first sandy and almost bare and then (at about 220 m from the primary vent) it is colonized by a sparse seagrass meadow that becomes progressively denser. *Cymodocea nodosa* is the only seagrass species and becomes mixed with *Zostera noltei* at a distance of about 400 m from the vent (Vizzini et al., 2017).

Despite Levante Bay is characterized by complex environmental gradients, which determine biogeochemical and microbial variability, this study substantiates the suitability of elemental content and stable isotopes to elucidate the origin and dynamics of SOM pool at small spatial scales and to show the spatial extent to which allochthonous input (*i.e.* volcanic) spread and may affect trophodynamic processes in the surrounding marine ecosystem. The assessment of the area influenced by volcanic emissions can guide experimental designs that investigate the effects of ocean acidification on various biological and ecological levels, as it supports the proper selection of study sites (*i.e.*, site with acidified conditions with a clear influence of the vent but without any bias from abiotics other than pH, such as volcanic-derived sulphur and toxic compounds, and control sites at distance from the vent where the volcanic influence is not detectable anymore).

While the effects of sediment features on the overlying communities are well understood, this study suggests that the role of benthic communities and their shifts on the spatial dynamics of SOM(in terms of origin, composition and quality) may also be worthy of further investigation because of rebounds on biota and implications on the complex and biunivocal interactions sediment-biota.

## 5. Conclusions

The peculiar abiotic features and the strong environmental spatial gradients driven by the volcanic emission of the shallow $CO_2$ vent at Levante Bay (Aeolian Archipelago, Tyrrhenian Sea, Italy) represent important drivers of the distribution and the abundance of benthic prokaryotic communities along the bay, revealing a marked biocomplexity at small spatial scales. Accordingly, strong gradients in the SOM composition and origin were highlighted by the analysis of the elemental and isotopic composition. A high influence of the volcanic emissions was evident up to about 350 m from the primary $CO_2$ vent, where the contribution of volcanic vent-derived organic matter sources to the sedimentary pool was high and exceeded the contribution of marine sources. This trend reversed at a greater distance, with a dominant contribution of marine sources. This is likely to have wide-ranging significances, from local-scale influences on the structure of benthic communities to larger-scale effects on the food-web structure and biogeochemical cycles, and relevant implications of correct site-selection for ocean acidification studies.

## CRediT authorship contribution statement

**C. Andolina:** Writing – review & editing, Writing – original draft, Visualization, Formal analysis. **G. Cilluffo:** Writing – review & editing, Writing – original draft, Visualization, Formal analysis. **V. Zammuto:** Writing – review & editing, Writing – original draft, Visualization, Validation, Investigation, Formal analysis. **G. Signa:** Writing – review & editing. **M. Papale:** Writing – original draft, Visualization, Validation, Investigation, Formal analysis. **A. Lo Giudice:** Writing – review & editing, Supervision, Methodology. **R. Di Leonardo:** Writing – original draft, Investigation. **V. Costa:** Writing – original draft, Investigation. **L. Ciriminna:** Writing – review & editing. **A. Tomasello:** Writing – review & editing, Supervision. **C. Gugliandolo:** Writing – review & editing, Supervision, Methodology, Funding acquisition. **S. Vizzini:** Writing – review & editing, Writing – original draft, Supervision, Resources, Project administration, Funding acquisition, Conceptualization.

## Declaration of competing interest

The authors declare that they have no known competing financial interests or personal relationships that could have appeared to influence the work reported in this paper.

## Acknowledgements

This paper has been supported by the projects “Mediterranean Sea Acidification under a changing climate-MedSeA” (EU FP7, grant agreement no. 265103) and has received funding from the European Union – NextGenerationEU, through the Italian Ministry of University and Research under PNRR (National Recovery and Resilience Plan – NRRP, Mission 4, Component 2, Investment 1.3 – D.D. 1243 August 2, 2022, PE0000005 – CUP: B73C22001220006) in the framework of the RETURN Extended Partnership. The views and opinions expressed are those of the authors only and do not necessarily reflect those of the European Union or the European Commission. Neither the European Union nor the European Commission can be held responsible for them. The authors would like to express sincere thanks to A. Savona for his support in field activities and to A.E. Aleo for laboratory analysis.

## Appendix A

**Table A1**
Mean proportional contribution (± s.d.) of organic matter sources to SOM at increasing distance from the primary vent, based on Bayesian mixing models estimates.

| Distance from primary vent | Microbial mats | SPOM-L | SPOM-C | Seagrasses |
|---|---|---|---|---|
| 0 | 0.70 ± 0.06 | 0.08 ± 0.05 | 0.17 ± 0.05 | 0.05 ± 0.02 |
| 5 | 0.93 ± 0.04 | 0.02 ± 0.02 | 0.03 ± 0.02 | 0.02 ± 0.02 |
| 25 | 0.90 ± 0.05 | 0.04 ± 0.04 | 0.04 ± 0.03 | 0.01 ± 0.01 |
| 50 | 0.89 ± 0.04 | 0.03 ± 0.03 | 0.05 ± 0.03 | 0.03 ± 0.02 |
| 75 | 0.82 ± 0.06 | 0.07 ± 0.06 | 0.09 ± 0.05 | 0.03 ± 0.02 |
| 100 | 0.79 ± 0.05 | 0.04 ± 0.04 | 0.08 ± 0.05 | 0.09 ± 0.04 |
| 150 | 0.54 ± 0.06 | 0.10 ± 0.09 | 0.26 ± 0.09 | 0.11 ± 0.05 |
| 178 | 0.51 ± 0.12 | 0.20 ± 0.17 | 0.26 ± 0.13 | 0.04 ± 0.03 |
| 200 | 0.54 ± 0.07 | 0.10 ± 0.10 | 0.28 ± 0.09 | 0.08 ± 0.05 |
| 227 | 0.38 ± 0.14 | 0.35 ± 0.24 | 0.23 ± 0.15 | 0.03 ± 0.03 |
| 250 | 0.45 ± 0.07 | 0.11 ± 0.10 | 0.30 ± 0.11 | 0.14 ± 0.07 |
| 272 | 0.30 ± 0.10 | 0.19 ± 0.18 | 0.46 ± 0.16 | 0.05 ± 0.04 |
| 300 | 0.38 ± 0.08 | 0.11 ± 0.11 | 0.33 ± 0.12 | 0.18 ± 0.08 |
| 350 | 0.41 ± 0.08 | 0.11 ± 0.10 | 0.32 ± 0.12 | 0.16 ± 0.08 |
| 396 | 0.27 ± 0.09 | 0.13 ± 0.14 | 0.54 ± 0.14 | 0.06 ± 0.05 |
| 400 | 0.45 ± 0.11 | 0.15 ± 0.15 | 0.34 ± 0.13 | 0.06 ± 0.05 |
| 450 | 0.34 ± 0.09 | 0.11 ± 0.11 | 0.37 ± 0.15 | 0.18 ± 0.10 |
| 500 | 0.20 ± 0.08 | 0.09 ± 0.09 | 0.56 ± 0.15 | 0.16 ± 0.10 |
| 511 | 0.13 ± 0.07 | 0.08 ± 0.09 | 0.74 ± 0.12 | 0.05 ± 0.05 |

## Data availability

Data will be made available on request.

## References

Altabet, M.A., 2006. Isotopic tracers of the marine nitrogen cycle: present and past. Handb. Environ. Chem. Vol. 2 react. Process. 2 N, 251–293. doi:https://doi.org/10.1007/698_2_008.

Antranikian, G., Suleiman, M., Schäfers, C., Adams, M.W.W., Bartolucci, S., Blamey, J. M., Birkeland, N.-K., Bonch-Osmolovskaya, E., da Costa, M.S., Cowan, D., et al., 2017. Diversity of bacteria and archaea from two shallow marine hydrothermal vents from Vulcano Island. Extremophiles 21, 733–742. https://doi.org/10.1007/s00792-017-0938-y.

Apostolaki, E.T., Vizzini, S., Hendriks, I.E., Olsen, Y.S., 2014. Seagrass ecosystem response to long-term high $CO_2$ in a Mediterranean volcanic vent. Mar. Environ. Res. 99, 9–15. https://doi.org/10.1016/j.marenvres.2014.05.008.

Arnold, T.M., Mealey, C., Leahey, H., Miller, A.W., Hall-Spencer, J.M., Milazzo, M., Maers, K., 2012. Ocean acidification and the loss of phenolic substances in marine plants. PLoS One 7, 10. https://doi.org/10.1371/journal.pone.0035107.

Baggini, C., Salomidi, M., Voutsinas, E., Bray, L., Krasakopoulou, E., Hall-Spencer, J.M., 2014. Seasonality affects macroalgal community response to increases in $pCO_2$. PLoS One 9, e106520. https://doi.org/10.1371/journal.pone.0106520.

Boatta, F., D'Alessandro, W., Gagliano, A.L., Liotta, M., Milazzo, M., Rodolfo-Metalpa, R., Hall-Spencer, J.M., Parello, F., 2013. Geochemical survey of Levante Bay, Vulcano Island (Italy), a natural laboratory for the study of ocean acidification. Mar. Pollut. Bull. 73, 485–494. https://doi.org/10.1016/j.marpolbul.2013.01.029.

Böttcher, M.E., Khim, B.K., Suzuki, A., Gehre, M., Wortmann, U.G., Brumsack, H.J., 2004. Microbial sulfate reduction in deep sediments of the Southwest Pacific (ODP leg 181, sites 1119-1125): evidence from stable sulfur isotope fractionation and pore water modeling. Mar. Geol. 205, 249–260. https://doi.org/10.1016/S0025-3227(04)00026-X.

Brandes, J.A., Devol, A.H., 1997. Isotopic fractionation of oxygen and nitrogen in coastal marine sediments. Geochim. Cosmochim. Acta 61, 1793–1801. https://doi.org/10.1016/S0016-7037(97)00041-0.

Campbell, B.J., Engel, A.S., Porter, M.L., Takai, K., 2006. The versatile ε-proteobacteria: Key players in sulphidic habitats. Nat. Rev. Microbiol. 4, 458–468. https://doi.org/10.1038/nrmicro1414.

Capaccioni, B., Tassi, F., Vaselli, O., 2001. Organic and inorganic geochemistry of low temperature gas discharges at the Baia di Levante beach, Vulcano Island. Italy. J. Volcanol. Geotherm. Res. 108, 173–185. https://doi.org/10.1016/S0377-0273(00)00284-5.

Casamayor, E.O., Schafer, H., Baneras, L., Pedro's-Alio, C., Muyzer, G., 2000. Identification of and spatio-temporal difference between microbial assemblages from two neighboring Sulphur lakes: comparison by microscopy and denaturing gradient gel electrophoresis. Appl. Environ. Microbiol. 66, 499–508. https://doi.org/10.1128/AEM.66.2.499-508.2000.

Dando, P.R., Stüben, D., Varnavas, S.P., 1999. Hydrothermalism in the Mediterranean Sea. Prog. Oceanogr. 44, 333–367. https://doi.org/10.1016/S0079-6611(99)00032-4.

De Leeuw, J., Frewin, N.L., Van Bergen, P.F., Sinninghe Damsté, J.S., Collinson, M.E., 1995. Organic carbon as a palaeoenvironmental indicator in the marine realm. Geol. Soc. London. Spec. Publ. 83, 43–71. https://doi.org/10.1144/GSL.SP.1995.083.01.04.

Fagerbakke, K.M., Heldal, M., Norland, S., 1996. Content of carbon, nitrogen, oxygen, sulfur and phosphorus in native aquatic and cultured bacteria. Aquat. Microb. Ecol. 10, 15–27. https://doi.org/10.3354/ame010015.

Giovannelli, D., D'Errico, G., Manini, E., Yakimov, M., Vetriani, C., 2013. Diversity and phylogenetic analyses of bacteria from a shallow-water hydrothermal vent in Milos Island (Greece). Front. Microbiol. 4, 1–13. https://doi.org/10.3389/fmicb.2013.00184.

Gong, C., Hollander, D., 1997. Differential contribution of bacteria to sedimentary organic matter in oxic and anoxic environments, Santa Monica Basin. California. Org. Geochem. 26, 545–563. https://doi.org/10.1016/S0146-6380(97)00018-1.

Gugliandolo, C., Italiano, F., Maugeri, T.L., 2006. The submarine hydrothermal system of Panarea (southern Italy): biogeochemical processes at the thermal fluids-sea bottom interface. Ann. Geophys. 49, 783–792. https://doi.org/10.4401/ag-3139.

Gugliandolo, C., Lentini, V., Bunk, B., Overmann, J., Italiano, F., Maugeri, T.L., 2015. Changes in prokaryotic community composition accompanying a pronounced temperature shift of a shallow marine thermal brine pool (Panarea Island, Italy). Extremophiles 19, 547–559. https://doi.org/10.1007/s00792-015-0737-2.

Gugliandolo, C., Lentini, V., Spanò, A., Maugeri, T.L., 2012. New bacilli from shallow hydrothermal vents of Panarea Island (Italy) and their biotechnological potential. J. Appl. Microbiol. 112, 1102–1112. https://doi.org/10.1111/j.1365-2672.2012.05272.x.

Gugliandolo, C., Maugeri, T.L., 1993. Chemolithotrophic, sulfur-oxidizing bacteria from a marine, shallow hydrothermal vent of Vulcano (Italy). Geomicrobiol. J. 11, 109–120. https://doi.org/10.1080/01490459309377939.

Gugliandolo, C., Maugeri, T.L., 1998. Temporal variations in heterotrophic mesophilic bacteria from a marine shallow hydrothermal vent off the island of Vulcano (Eolian Islands, Italy). Microb. Ecol. 36, 13–22. https://doi.org/10.1007/s002489900088.

Gugliandolo, C., Maugeri, T.L., 2019. Phylogenetic diversity of Archaea in shallow hydrothermal vents of Eolian Island. Italy. Diversity 11, 156. https://doi.org/10.3390/d11090156.

Hall-Spencer, J.M., Rodolfo-Metalpa, R., Martin, S., Ransome, E., Fine, M., Turner, S.M., Rowley, S.J., Tedesco, D., Buia, M.C., 2008. Volcanic carbon dioxide vents show ecosystem effects of ocean acidification. Nature 454, 96–99. https://doi.org/10.1038/nature07051.

Hirayama, H., Sunamura, M., Takai, K., Nunoura, T., Noguchi, T., Oida, H., Furushima, Y., Yamamoto, H., Oomori, T., Horikoshi, K., 2007. Culture-dependent and -independent characterization of microbial communities associated with a shallow submarine hydrothermal system occurring within a coral reef off Taketomi Island. Japan. Appl. Environ. Microbiol. 73, 7642–7656. https://doi.org/10.1128/AEM.01258-07.

Hoegh-Guldberg, O., Cai, R., Poloczanska, E.S., Brewer, P.G., Sundby, S., Hilmi, K., Fabry, V.J., Jung, S., 2015. The Ocean, in: Climate Change 2014: Impacts, Adaptation and Vulnerability: Part B: Regional Aspects: Working Group II Contribution to the Fifth Assessment Report of the Intergovernmental Panel on Climate Change. https://doi.org/10.1017/CBO9781107415386.010.

Inagaki, F., Takai, K., Nealson, K.H., Horikoshi, K., 2004. *Sulfurovum lithotrophicum* gen. Nov., sp. nov., a novel sulfur-oxidizing chemolithoautotroph within the *epsilon-proteobacteria* isolated from Okinawa trough hydrothermal sediments. Int. J. Syst. Evol. Microbiol. 54, 1477–1482. https://doi.org/10.1099/ijs.0.03042-0.

Italiano, F., Nuccio, P.M., 1991. Geochemical investigations of submarine volcanic exhalations to the east of Panarea, Aeolian Islands. Italy. J. Volcanol. Geotherm. Res. 46, 125–141. https://doi.org/10.1016/0377-0273(91)90079-F.

Karl, D., Michaels, A., Bergman, B., Capone, D., Carpenter, E., Letelier, R., Lipschultz, F., Paerl, H., Sigman, D., Stal, L., 2002. Dinitrogen fixation in the world's oceans. Biogeochemistry 57–58, 47–98. https://doi.org/10.1023/A:1015798105851.

Kirchman, D.L., 2002. The ecology of Cytophaga-Flavobacteria in aquatic environments. FEMS Microbiol. Ecol. 39, 91–100. https://doi.org/10.1016/S0168-6496(01)00206-9.

Lentini, V., Gugliandolo, C., Bunk, B., Overmann, J., Maugeri, T.L., 2014. Diversity of prokaryotic community at a shallow marine hydrothermal site elucidated by illumina sequencing technology. Curr. Microbiol. 69, 457–466. https://doi.org/10.1007/s00284-014-0609-5.

Lepoint, G., Dauby, P., Gobert, S., 2004. Applications of C and N stable isotopes to ecological and environmental studies in seagrass ecosystems. Mar. Pollut. Bull. 49, 887–891. https://doi.org/10.1016/j.marpolbul.2004.07.005.

Martínez-Crego, B., Vizzini, S., Califano, G., Massa-Gallucci, A., Andolina, C., Gambi, M. C., Santos, R., 2020. Resistance of seagrass habitats to ocean acidification via altered interactions in a tri-trophic chain. Sci. Rep. 10 (1), 5103. https://doi.org/10.1038/s41598-020-61753-1.

Maugeri, T.L., Lentini, V., Gugliandolo, C., Cousin, S., Stackebrandt, E., 2010. Microbial diversity at a hot, shallow-sea hydrothermal vent in the southern Tyrrhenian Sea (Italy). Geomicrobiol J. 27, 380–390. https://doi.org/10.1080/01490450903451518.

Maugeri, T.L., Lentini, V., Gugliandolo, C., Italiano, F., Cousin, S., Stackebrandt, E., 2009. Bacterial and archaeal populations at two shallow hydrothermal vents off Panarea Island (Eolian Islands, Italy). Extremophiles 13, 199–212. https://doi.org/10.1007/s00792-008-0210-6.

Maugeri, T.L., Lentini, V., Spanò, A., Gugliandolo, C., 2013. Abundance and diversity of picocyanobacteria in shallow hydrothermal vents of Panarea Island (Italy). Geomicrobiol J. 30, 93–99. https://doi.org/10.1080/01490451.2011.653088.

Mehta, M.P., Baross, J.A., 2006. Nitrogen fixation at 92°C by a hydrothermal vent archaeon. Science 314, 1783–1786. https://doi.org/10.1126/science.1134772.

Meyers, P., 1997. Organic geochemical proxies of paleoceanographic, paleolimnologic, and paleoclimatic processes. Org. Geochem. 27, 213–250. https://doi.org/10.1016/S0146-6380(97)00049-1.

Michener, R.H., Kaufman, L., 2007. Stable isotope ratios as tracers in marine food webs: An update. In: Michener, R., Lajtha, K. (Eds.), Stable Isotopes in Ecology and Environmental Science, Second edition. Blackwell Publishing Ltd, pp. 238–282. https://doi.org/10.1002/9780470691854.ch9.

Mostofa, K.M.G., Liu, C.Q., Zhai, W.D., Minella, M., Vione, D., Gao, K., Minakata, D., Arakaki, T., Yoshioka, T., Hayakawa, K., Konohira, E., Tanoue, E., Akhand, A., Chanda, A., Wang, B., Sakugawa, H., 2015. Reviews and syntheses: ocean acidification and its potential impacts on marine ecosystems. Biogeosci. Discuss. 12, 10939–10983. https://doi.org/10.5194/bgd-12-10939-2015.

Muyzer, G., De Waal, E.C., Uitterlinden, A.G., 1993. Profiling of complex microbial populations by denaturing gradient gel electrophoresis analysis of polymerase chain reaction-amplified genes coding for 16S rRNA. Appl. Environ. Microbiol. 59, 695–700. https://doi.org/10.1128/aem.59.3.695-700.1993.

Muyzer, G., Hottenträger, S., Teske, A., Wawer, C., 1996. Denaturing gradient gel electrophoresis of PCR-amplified 16S rDNA - A new molecular approach to analyse the genetic diversity of mixed microbial communities. In: Akkermans, A.D.L., van Elsas, J.D., de Bruijn, F.J. (Eds.), Molecular Microbial Ecology Manual, 3.4.4. Kluwer Academic Publishers, Dordrecht, The Netherlands, pp. 1–23.

Noè, S., Bellavia, C., Calvo, S., Mazzola, A., Pirrotta, M., Sciandra, M., Vizzini, S., Tomasello, A., 2020. Resilience of the seagrass *Posidonia oceanica* following pulse-type disturbance. Mar. Environ. Res. 159, 105011. https://doi.org/10.1016/j.marenvres.2020.105011.

Orr, J.C., Fabry, V.J., Aumont, O., Bopp, L., Doney, S.C., Feely, R.A., Gnanadesikan, A., Gruber, N., Ishida, A., Joos, F., Key, R.M., Lindsay, K., Maier-Reimer, E., Matear, R., Monfray, P., Mouchet, A., Najjar, R.G., Plattner, G.K., Rodgers, K.B., Sabine, C.L., Sarmiento, J.L., Schlitzer, R., Slater, R.D., Totterdell, I.J., Weirig, M.F., Yamanaka, Y., Yool, A., 2005. Anthropogenic Ocean acidification over the twenty-first century and its impact on calcifying organisms. Nature 437, 681–686. https://doi.org/10.1038/nature04095.

Papadimitriou, S., Kennedy, H., Kennedy, D.P., Duarte, C.M., Marbà, N., 2005. Sources of organic matter in seagrass-colonized sediments: a stable isotope study of the silt and clay fraction from Posidonia oceanica meadows in the western Mediterranean. Org. Geochem. 36, 949–961. https://doi.org/10.1016/j.orggeochem.2004.12.002.

Patwardhan, S., Foustoukos, D.I., Giovannelli, D., Yücel, M., Vetriani, C., 2018. Ecological succession of sulfur-oxidizing epsilon-and Gammaproteobacteria during colonization of a shallow-water gas vent. Front. Microbiol. 9, 2970. https://doi.org/10.3389/fmicb.2018.02970.

Pernthaler, J., Glöckner, F.O., Schönhuber, W., Amann, R., 2001. Fluorescence in situ hybridization (FISH) with rRNA-targeted oligonucleotide probes. Methods Microbiol. 30, 207–226. https://doi.org/10.1016/s0580-9517(01)30046-6.

Peterson, B., Howarth, R., 1987. Sulfur, carbon, and nitrogen isotopes used to trace organic matter flow in the salt-marsh estuaries of Sapelo Island. Georgia. Limnol. Oceanogr. 32, 1195–1213. https://doi.org/10.2307/1939809.

Peterson, B.J., Fry, B., 1987. Stable isotopes in ecosystem studies. Annu. Rev. Ecol. Syst. 18, 293–320. https://doi.org/10.1146/annurev.es.18.110187.001453.

Porzio, L., Buia, M.C., Hall-Spencer, J.M., 2011. Effects of ocean acidification on macroalgal communities. J. Exp. Mar. Biol. Ecol. 400, 278–287. https://doi.org/10.1016/j.jembe.2011.02.011.

Price, R.E., Giovannelli, D., 2017. A Review of the Geochemistry and Microbiology of Marine Shallow-Water Hydrothermal Vents. in Reference Module in Earth Systems and Environmental Sciences. https://doi.org/10.1016/b978-0-12-409548-9.09523-3.

R Core Team, 2018. R: A Language and Environment for Statistical Computing. R Foundation for Statistical Computing, Vienna, Austria. Available online at: https://www.R-project.org/.

Rees, C.E., Jenkins, W.J., Monster, J., 1978. The Sulphur isotopic composition of ocean water sulphate. Geochim. Cosmochim. Acta 42, 377–381. https://doi.org/10.1016/0016-7037(78)90268-5.

Ricevuto, E., Vizzini, S., Gambi, M.C., 2015. Ocean acidification effects on stable isotope signatures and trophic interactions of polychaete consumers and organic matter sources at a $CO_2$ shallow vent system. J. Exp. Mar. Biol. Ecol. 468, 105–117. https://doi.org/10.1016/j.jembe.2015.03.016.

Rona, P.A., Scott, S.D., 1993. A special issue on sea-floor hydrothermal mineralization; new perspectives; preface. Econ. Geol. 88, 1935–1976. https://doi.org/10.2113/gsecongeo.88.8.1935.

Russell, B.D., Connell, S.D., Uthicke, S., Muehllehner, N., Fabricius, K.E., Hall-Spencer, J. M., 2013. Future seagrass beds: Can increased productivity lead to increased carbon storage? Mar. Pollut. Bull. 73 (2), 463–469. https://doi.org/10.1016/j.marpolbul.2013.01.031.

Sieland, R., Steinbrückner, D., Hamel, M., Merkel, B., Schipek, M., 2009. Geochemical investigations and gas quantification of submarine fluid discharges in the hydrothermal system of Panarea (Aeolian Islands, Italy). FOG - Freib. Online Geosci. 22, 87–93.

Signa, G., Mazzola, A., Vizzini, S., 2012. Effects of a small seagull colony on trophic status and primary production in a Mediterranean coastal system (Marinello ponds, Italy). Estuar. Coast. Shelf Sci. 111, 27–34. https://doi.org/10.1016/j.ecss.2012.06.008.

Steinbrückner, D., 2009. Quantification of submarine degassing of Panarea volcano in the Aeolian archipelago. Italy. FOG - Freib. Online Geosci. 23, 6–11.

Stock, B., Semmens, B., 2013. MixSIAR GUI User Manual: version 1.0.

Stock, B.C., Jackson, A.L., Ward, E.J., Parnell, A.C., Phillips, D.L., Semmens, B.X., 2018. Analyzing mixing systems using a new generation of Bayesian tracer mixing models. PeerJ 6, e5096. https://doi.org/10.7717/peerj.5096.

Strauss, H., 1997. The isotopic composition of sedimentary sulfur through time. Palaeogeogr. Palaeoclimatol. Palaeoecol. 132, 97–118. https://doi.org/10.1016/S0031-0182(97)00067-9.

Svensson, E., Skoog, A., Amend, J.P., 2004. Concentration and distribution of dissolved amino acids in a shallow hydrothermal system, Vulcano Island (Italy). Org. Geochem. 35, 1001–1014. https://doi.org/10.1016/j.orggeochem.2004.05.005.

Tarasov, V.G., 2006. Effects of shallow-water hydrothermal venting on biological communities of coastal marine ecosystems of the western Pacific. Adv. Mar. Biol. 50, 267–421. https://doi.org/10.1016/S0065-2881(05)50004-X.

Tarasov, V.G., Gebruk, A.V., Mironov, A.N., Moskalev, L.I., 2005. Deep-sea and shallow-water hydrothermal vent communities: two different phenomena? Chem. Geol. 224, 5–39. https://doi.org/10.1016/j.chemgeo.2005.07.021.

Ullah, H., Nagelkerken, I., Goldenberg, S.U., Fordham, D.A., 2018. Climate change could drive marine food web collapse through altered trophic flows and cyanobacterial proliferation. PLoS Biol. 16. https://doi.org/10.1371/journal.pbio.2003446.

Vetriani, C., Voordeckers, J.W., Crespo-Medina, M., O'Brien, C.E., Giovannelli, D., Lutz, R.A., 2014. Deep-sea hydrothermal vent Epsilonproteobacteria encode a conserved and widespread nitrate reduction pathway (nap). ISME J. 8, 1510–1521. https://doi.org/10.1038/ismej.2013.246.

Vizzini, S., Apostolaki, E.T., Ricevuto, E., Polymenakou, P., Mazzola, A., 2019. Plant and sediment properties in seagrass meadows from two Mediterranean $CO_2$ vents: implications for carbon storage capacity of acidified oceans. Mar. Environ. Res. 146, 101–108. https://doi.org/10.1016/j.marenvres.2019.03.001.

Vizzini, S., Di Leonardo, R., Costa, V., Tramati, C.D., Luzzu, F., Mazzola, A., 2013. Trace element bias in the use of $CO_2$ vents as analogues for low pH environments: implications for contamination levels in acidified oceans. Estuar. Coast. Shelf Sci. 134, 19–30. https://doi.org/10.1016/j.ecss.2013.09.015.

Vizzini, S., Martínez-Crego, B., Andolina, C., Massa-Gallucci, A., Connell, S.D., Gambi, M. C., 2017. Ocean acidification as a driver of community simplification via the collapse of higher-order and rise of lower-order consumers. Sci. Rep. 7, 1–10. https://doi.org/10.1038/s41598-017-03802-w.

Vizzini, S., Tomasello, A., Maida, G., Di Pirrotta, M., Mazzola, A., Calvo, S., 2010. Effect of explosive shallow hydrothermal vents on δ13C and growth performance in the seagrass *Posidonia oceanica*. J. Ecol. 98, 1284–1291. https://doi.org/10.1111/j.1365-2745.2010.01730.x.